



Universiteit
Leiden
The Netherlands

In vivo high field magnetic resonance imaging and spectroscopy of adult zebrafish

Kabli, S.

Citation

Kabli, S. (2009, October 7). *In vivo high field magnetic resonance imaging and spectroscopy of adult zebrafish*. Retrieved from <https://hdl.handle.net/1887/14040>

Version: Corrected Publisher's Version

License: [Licence agreement concerning inclusion of doctoral thesis in the Institutional Repository of the University of Leiden](#)

Downloaded from: <https://hdl.handle.net/1887/14040>

Note: To cite this publication please use the final published version (if applicable).

3 *In Vivo* Metabolite Profile of Adult Zebrafish Brain Obtained by High Resolution Localized Magnetic Resonance Spectroscopy*

3.1 Abstract

Zebrafish (*Danio rerio*) is increasingly used as a model organism for understanding brain diseases including neurodegenerative disorders owing to their similar organization of brain components as that of human. However, investigating the brain metabolites of adult zebrafish *in vivo* has not yet been possible. In this study we have implemented and optimized high resolution localized ^1H Magnetic resonance spectroscopy (MRS) at 9.4T and obtained for the first time *in vivo* localized MR spectra from zebrafish brain. High resolution spectra were obtained from a voxel as small as 3.3 μl placed in the middle of the zebrafish brain. Excellent separation of resonances from various metabolites was achieved *in vivo*. In addition, a two dimensional homonuclear correlation spectrum of the zebrafish brain extracts was measured to get a comprehensive metabolic profile of adult zebrafish brain. This study suggests that zebrafish brain has a very similar metabolite profile as the human brain, which proves that zebrafish is a good

**This chapter was published in J Magn Reson Imaging 2009; 29:275-281*

organism for human brain disorders. Precise *in vivo* biochemical information from distinct regions of the zebrafish brain as obtained in this study can be invaluable for monitoring of disease progression and treatment as well as phenotyping of large number of available zebrafish models of various brain diseases.

3.2 Introduction

Although *in vivo* MR imaging and spectroscopy has become a versatile tool in medicine and pharmacological research (1, 2), very few studies use this method to uncover physiological and biochemical issues in aquatic organisms (3, 4). The zebrafish (*Danio rerio*) is assuming an ever increasing importance as a model for developmental and genetic manipulation studies (5-8). The embryos develop externally and are transparent, facilitating analysis of their development *in vivo*. In addition, the organism can be readily manipulated genetically using either forward or reverse genetic techniques to produce transgenic animals. A large number of zebrafish mutations have been described, many of which phenocopy many human disorders (8). *In vivo* studies of zebrafish are however, mainly restricted to early stages because of the opaqueness of adult phase which cannot be approached by optical imaging methods. Recently *in vivo* μ MRI methods have been optimized to image live adult zebrafish with a 9.4T MRI scanner (9) and sufficient anatomical details from adult zebrafish have been resolved using T_2 weighted fast spin echo sequences.

Zebrafish is also increasingly used as an important model system for understanding the vertebrate central nervous system and brain development (10-12). The basic organization of zebrafish brain is similar to other vertebrate brains (13). The modulatory neurotransmitter system in zebrafish

is highly similar to mammalian systems (14). Considerable knowledge concerning the embryonic development of the brain of zebrafish has accumulated in recent years using optical microscopic imaging methods (15). However, there is an apparent lack of information on the structural organization and neurochemical composition of adult zebrafish brain *in vivo*. While many zebrafish mutants of the central nervous system are available, the molecular mechanism that is operative in many cases is not very well known. The relevance of zebrafish models for human brain diseases should be validated *in vivo*, not only at early embryonic stages but also at adult stage when the brain is fully functional.

The brain metabolites are sensitive to various pathological processes at the molecular or cellular level. For example, N-acetylaspartate (NAA) is believed to be a marker for neuronal number and health, glutamate (Glu) acts as an excitatory neurotransmitter, and myo-inositol (mIns) is thought to be a marker for osmotic stress or astrogliosis (16,17). A comprehensive picture of the metabolites of zebrafish brain is apparently lacking, while neurochemical information of the adult zebrafish brain *in vivo* may be indispensable to follow changes during disease progression at the molecular level. Magnetic resonance spectroscopy (MRS) is one of the few available techniques that, in principle, can provide *in vivo* information on the neurochemistry of zebrafish non-invasively. However, due to the very small size of adult zebrafish brain (5-6 mm), application of MRS in zebrafish will be highly challenging. In addition, being a small aquatic animal, zebrafish requires a special setup and several precautions for supporting *in vivo* MR spectroscopy (9). In the present study we optimized high resolution localized ¹H-MR spectroscopic methods at 9.4T to get for the first time a localized MR spectrum from live zebrafish brain providing metabolite composition of the zebrafish brain *in vivo*. In addition, an

extensive metabolic profile of adult zebrafish was obtained using two dimensional homonuclear correlation spectroscopy of zebrafish brain extracts. The *in vivo* ^1H MRS methods developed in this work for zebrafish brain can be applied in the future to study brain disorders using variety of available zebrafish models for brain diseases.

3.3 Materials and methods

Zebrafisch

Adult wild-type zebrafish (*Danio rerio*) were maintained in recirculating aquarium systems according to established rearing procedures (16). The water temperature was maintained at 28 $^{\circ}\text{C}$ with a flow rate of 150 L/min, with day/night light cycles (12h dark versus 12h light). The fish were fed twice daily with commercial flake food according to Westerfield (16). All fish were handled according to Institutional Animal Care and Use Committee guidelines.

Extraction of the brains metabolites

For extraction of brain metabolites from zebrafish a modified procedure of Suhartono *et al.* (17) has been used. Ten adult zebrafish were euthanized and their brains were carefully removed from the skull and immediately frozen in liquid nitrogen. The brains were crushed in 4 ml methanol and water (1:1). Subsequently 4 ml chloroform was added. The mixture was sonicated for 15 min followed by centrifugation at 5000 rpm at 4 $^{\circ}\text{C}$. After centrifugation two layers were formed: an upper chloroform layer and a lower methanol and water layer (aqueous layer). The two layers were carefully removed and dried under nitrogen flow at 4 $^{\circ}\text{C}$. The dried chloroform layer was dissolved in 1 ml d_4 chloroform and subsequently filtered using Millipore filter. The dried methanol and water layer was

dissolved in 100 mM KD_2PO_4 (pH 6.0) buffer containing 0.02% Trimethylsilylpropionic acid (TSP). This layer is referred to as the aqueous layer in the subsequent sections. Both samples were measured using 1D and 2D ^1H NMR.

Design of a flow-through chamber and experimental setup for in vivo spectroscopy

For *in vivo* $\mu\text{MRI/MRS}$ measurements, a fish was anaesthetised by adding 0.001% MS222 (ethyl meta aminobenzoate metanesulfonic acid salt; Sigma chemical co.) to pH controlled water. Subsequently the fish was transferred to a closed mini-flow-through chamber, which was specially designed to be fitted in a 10 mm volume RF coil to support the living zebrafish inside the magnet (Fig. 1a). The flow-through setup was placed in the centre of the volume coil (1 cm diameter, 4 cm length) (Fig. 1b) inside the microimaging probe, which was then inserted into the bore of the vertical MR magnet (400 MHz). Aerated water with anaesthetic was pumped from a temperature controlled aquarium to a tube entering to the flow-through cell, and opens close to the mouth of the fish. After passing the chamber the water was transported back to the aquarium. The setup allowed direct *in vivo* NMR measurements at constant flow speeds (10 ml/min) which were regulated by a STEPDOS 03/08 pump (KNF Flodos AG, Switzerland). After the MRI/MRS measurements, zebrafish were transferred back to normal aquarium without anaesthetic where fish recovered uneventfully from the experimental treatment within 1-2h.

Magnetic resonance microimaging/ spectroscopy

All measurements were conducted with a 400 MHz (9.4T) vertical bore system, using a transmit/receive birdcage radiofrequency coil with an inner diameter of 10 mm and a 1 Tm^{-1} gradient insert from Bruker Analytic,

Germany. The system was interfaced to a Linux operating system running Topspin 1.5 and Para Vision 4.0 imaging software (Bruker Biospin, Germany).

Localized T_2 - weighted multislice rapid acquisition with relaxation enhancement (RARE) (18) images were acquired to select a volume of interest (voxel). Basic measurement parameters used for the RARE sequence were; echo time (TE) = 15 ms; Repetition time (TR) = 1500 ms; RARE factor = 4. The field of view was 1.0 cm with an image matrix of 256×256 and the slice thickness was 0.2 mm. The MRS voxel ($1.5 \text{ mm} \times 1.5 \text{ mm} \times 1.5 \text{ mm}$) was localized in the centre of the zebrafish brain covering mainly cerebellum and mesencephalon and a small part of diencephalon and medulla. The local field homogeneity was optimized by adjustment of the first and second order shim coil current using the FASTMAP sequence (19). The field homogeneity resulted in a water line width of 20 – 25 Hz.

For 1D localized ^1H NMR spectroscopy, the PRESS (Point Resolved Spectroscopy) sequence was used (20). The sequence consists of 3 hermite RF pulses (90° , 180° , 180°). The TR and TE were 3500 ms and 10 ms respectively. As can be seen in Fig. 1c, the PRESS sequence was preceded by a VAPOR (Variable Pulse Power and Optimized Relaxation Delays) sequence for global water suppression (21) which consists of seven variable power RF pulses with an optimized relaxation delay. Outer volume suppression (OVS) was combined in an interleaved mode with the water suppression scheme, thus improving the localization performance and reducing the demands for spoiler gradients (Fig. 3.1). The OVS scheme used a total of 18 hyperbolic secant RF pulses, each with 90° nominal flip angle and 1 ms pulse length. The PRESS sequence used 2048 complex

points with a spectral width of 10 ppm. The final 1D datasets collected in 256 scans with a scan time of approximately 15 minutes.

Solution NMR measurements

Solution NMR spectra were recorded at 25 °C with a Bruker 400 MHz DMX NMR spectrometer equipped with a pulsed field gradient accessory (Bruker, Germany). 2D homonuclear ^1H - ^1H experiments were performed using the chemical shift correlated spectroscopic sequence (COSY) with a 5 mm inverse triple high resolution probe with actively shielded gradient coils. The ^1H shift was calibrated using TSP as an internal standard. To minimize the relaxation effect and enable reliable metabolite quantification, a repetition time of 3.7s was used during NMR measurements. The concentrations of the various metabolites in the brain extract were determined by comparing the integral peak intensity of the compounds of interest with that of the TSP peak, after correcting for the number of contributing protons and for tissue weight.

Quantification

The acquired *in vivo* spectra were analyzed by using LCModel (22, 23), which calculated the best fit of the experimental spectrum as a linear combination of model spectra. The final analysis is performed in the frequency domain; however, raw data (FIDs) are used as standard data input. The following metabolites were included in the basis set for LCModel: alanine (Ala), aspartate (Asp), creatine (Cr), γ -aminobutyric acid (GABA), glucose (Glc), glutamate (Glu), glutamine (Gln), glycerophosphocholine (GPC), phosphocholine (PCho), *myo*-inositol (Ins), lactate (Lac), N-acetylacetate (NAA), N-acetylaspartylglutamate (NAAG),

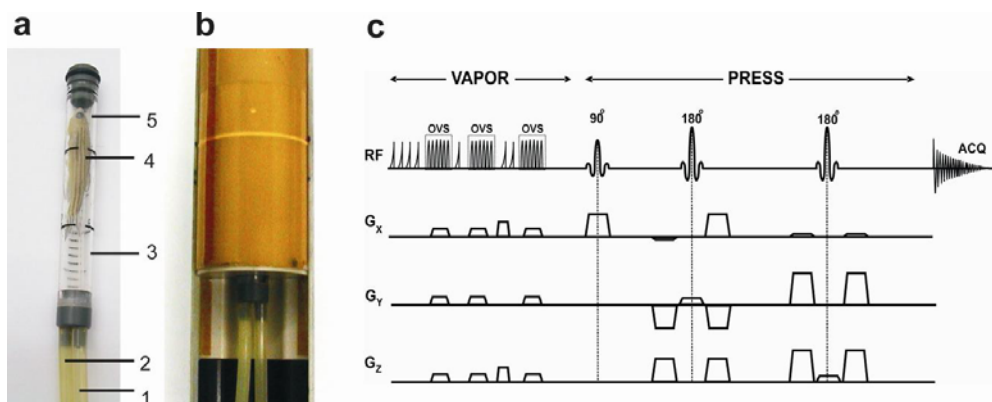


Figure 3.1 (a) Design of flow-through chamber for *in vivo* MRI/MRS measurement of living adult zebrafish. (1) water inlet; (2) water outlet; (3) PVC chamber (inner diameter 8 mm) which holds the fish; (4) a specimen of adult zebrafish; (5) water inlet inside the PVC tube which brings water near the mouth of the fish. (b) Flow-through chamber fitted into the volume coil (10 mm diameter) of the microimaging probe. (c) The PRESS pulse sequence used for localized *in vivo* MR spectroscopy of adult zebrafish brain. The PRESS sequence is preceded by VAPOR sequence for global water suppression interleaved with outer volume suppression (OVS).

phosphocreatine (PCr), phosphoethanolamine (PE), *scyllo*-inositol (sIns), and taurine (Tau). Quantification was obtained by using the tCr resonance as an internal standard. The LCModel fitting was performed over the spectral range from 1.0 to 4.4 ppm.

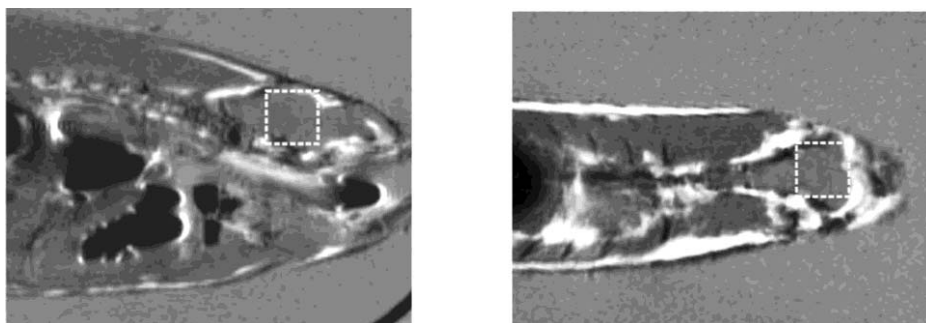
3.4 Results

3.4.1 *In vivo* proton MR spectroscopy of adult zebrafish brain

A small flow-through chamber designed to support imaging of living zebrafish is shown in Fig. 3.1a. This design is adapted from previous *in vivo* studies on zebrafish (9) and was modified so that it can fit into a 1cm RF coil to get high signal-to-noise ratio (SNR) from brain of zebrafish using

μ MRI and MRS. Figure 3.2A shows *in vivo* multislice RARE images of the adult zebrafish brain with a spatial resolution and contrast that guaranteed precise and reproducible placement of the selected volume of interest (voxel) in the center of the brain. Figure 3.2b shows a characteristic *in vivo* ^1H NMR spectrum obtained from the voxel as shown in Fig. 3.2a. Generally short echo time localization methods minimize T_2 relaxation effects, which increases the sensitivity and reliability of metabolite quantification (24). A short echo time of 10 ms was used for *in vivo* 2D MRS in the present study. The spectrum was acquired within 13 min at 9.4T which showed reasonable SNR, resolution and stability. This reasonably good resolution from such a small voxel of only 3.3 μl was accomplished by using FASTMAP automated shimming supported by an efficient shim system (19). In a 3.3 μl voxel, shimming routinely resulted in a unsuppressed water signal line width of 20–25 Hz. Efficient water suppression was achieved using a combination of 7 variable power RF pulses with optimized relaxation delays (Fig. 3.1b). The residual water signal was well below the level of most observable metabolites. Contamination by the signal arising from outside the volume of interest was minimized by outer volume saturation using a series of hyperbolic secant RF pulses, resulting in a sharp volume definition. As can be seen in Fig. 3.2b, in addition to the commonly observed NMR signals of methyl resonances of NAA, tCr, and Cho, characteristic spectral patterns of other metabolites, such as Glu, Gln, Ins and Tau were discernible in the *in vivo* ^1H NMR spectrum from the brain of

(A)



(B)

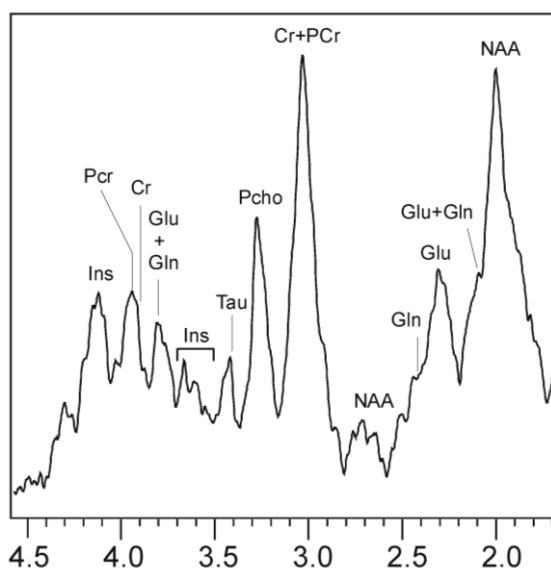


Figure 3.2 *In vivo* high resolution localized MR spectrum from zebrafish brain obtained at 9.4T. (A) MR image in the sagittal and axial planes through the head of living zebrafish, obtained by the RARE sequence with TR=1500ms and TE=15ms, showing the position of the selected voxel of $3.37 \mu\text{l}$ ($1.5 \times 1.5 \times 1.5 \text{ mm}^3$) covering most of the brain region. (B) One-dimensional localized MR spectrum from the selected $3.37 \mu\text{l}$ voxel in the zebrafish brain obtained by the PRESS sequence with TR=3500 ms and TE=15 ms. ^1H -chemical shifts in ppm.

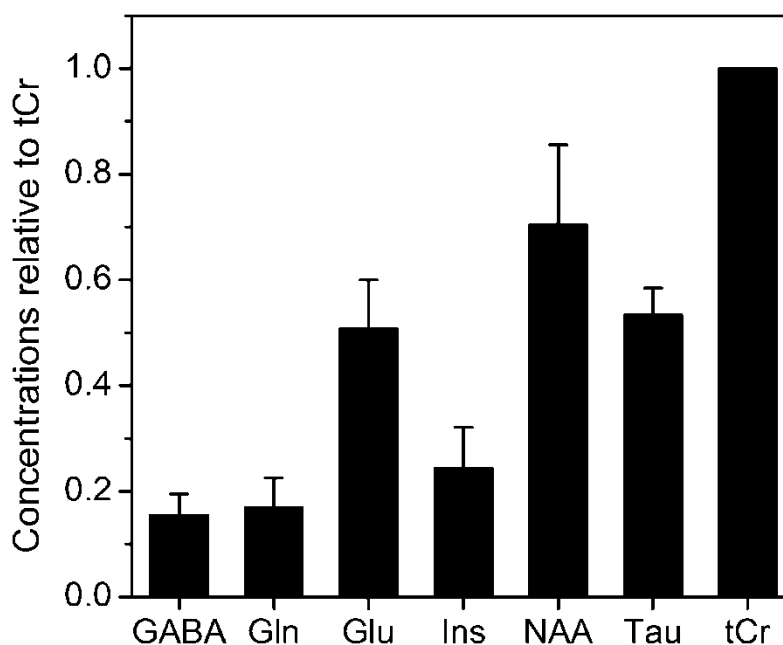


Figure 3.3 Concentrations of metabolites relative to tCr quantified by LCModel in the brain of living zebrafish ($n=4$).

living zebrafish. The *in vivo* ^1H NMR spectrum was analyzed with LCModel to obtain ratios of concentrations of various brain metabolites to tCr. Figure 3.3 shows the concentration of major metabolites in zebrafish brain obtained by LCModel.

3.4.2 *In vitro* proton NMR spectroscopy of the zebrafish brain extracts

To get a wider metabolic profile of zebrafish brain, a 1D ^1H -spectrum has been measured from the extracts of zebrafish brain.

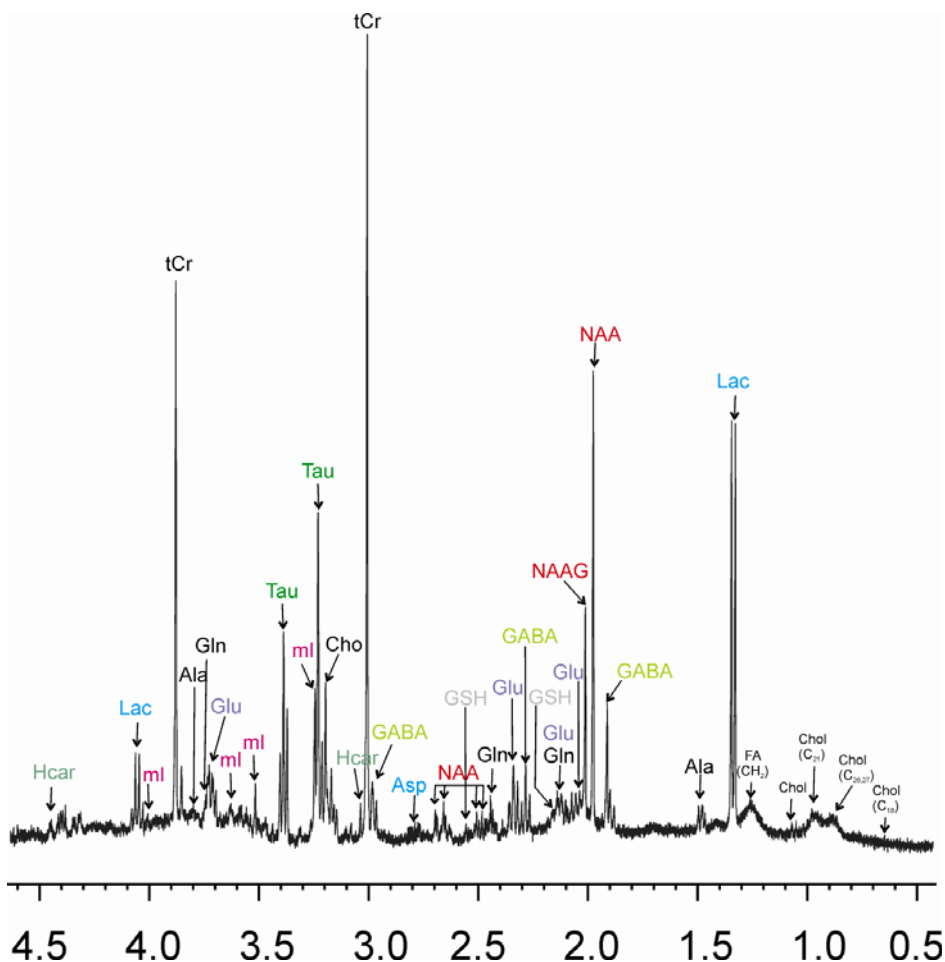


Figure 3.4 High resolution 1D ^1H spectrum of the brain extracts of zebrafish in KD_2PO_4 buffer containing 0.1% TSP. The spectrum was obtained at 25°C with a Bruker 400 MHz DMX NMR spectrometer (Bruker, Germany) using a 5 mm inverse triple high resolution probe with actively shielded two gradient coils. The ^1H shift was calibrated using TPS as an internal standard. Homocarnosine (HCar), lactate (Lac), myo-inositol (mI), total Creatin (tCr), alanine (Ala), glutamine (Gln), glutamate (Glu), taurine (Tau), choline (Cho), gamma-aminobutyric acid (GABA), N-acetyl-DL-aspartic acid (NAA), glutathione (GSH), N-acetylaspartylglutamate (NAAG), fatty acid (FA) and cholesterol (Chol).

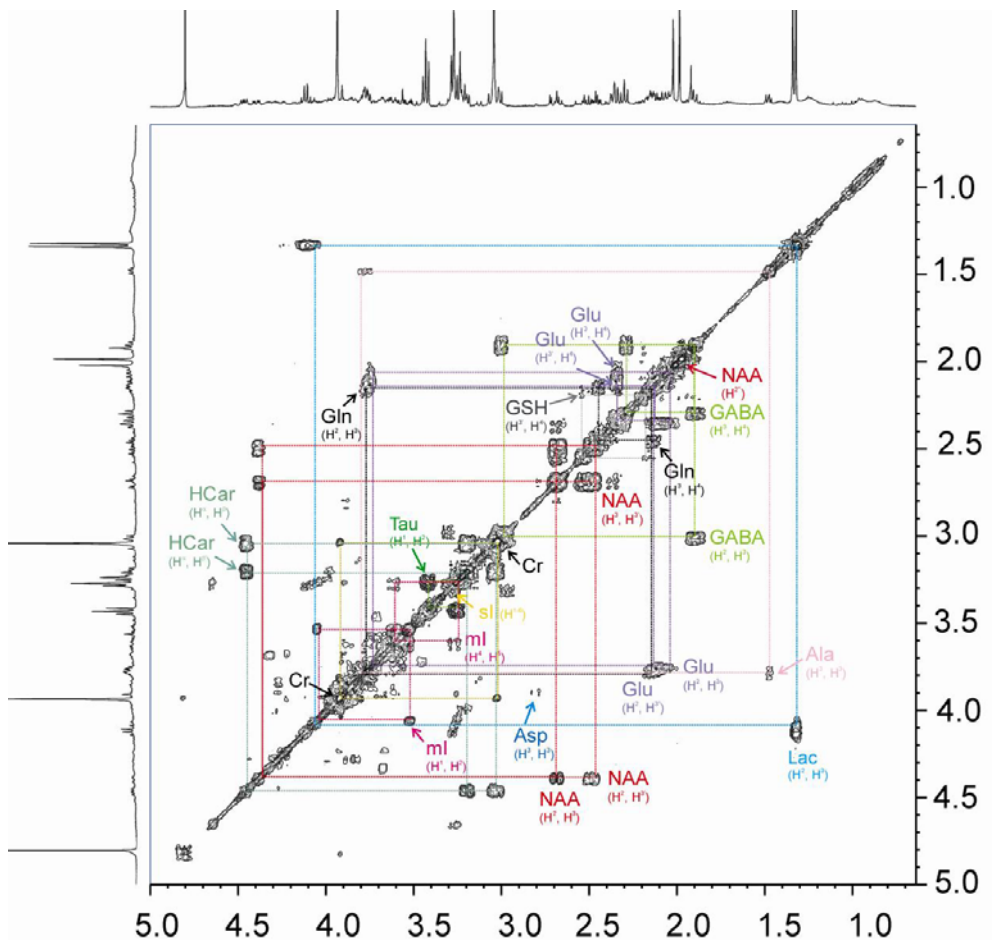


Figure 3.5 High resolution 2D [^1H - ^1H] homonuclear correlation spectrum of the brain extracts of zebrafish obtained at 25°C with a Bruker 400 MHz DMX NMR spectrometer (Bruker, Germany) using a 5 mm inverse triple high resolution probe with an actively shielded two gradient coils. The ^1H shift was calibrated using TPS as an internal standard. ^1H -chemical shifts in ppm.

Figure 3.4 shows the 1D ^1H -spectrum of the aqueous layer of the zebrafish brain extract which was better resolved than *in vivo* spectra and thus allows a more precise assignment of peak identities. In addition to the characteristic metabolites (NAA, Glu, Gln, Tau, tCr and Ins and GABA) that were

recognized in the *in vivo* spectra, many other metabolites such as Lac, Ala, NAAG, homocarnosine (HCar), choline (Cho) and glutathione (GSH), could be reliably measured in the zebrafish brain extracts by 1D ^1H NMR. The one dimensional ^1H spectrum of the brain extracts of zebrafish (Fig. 3.4) shows also a few signals in the lipids region from 0.6 ppm to 1.5 ppm, which were assigned to fatty acids and cholesterol. For the unambiguous assignment of the metabolite resonances in zebrafish brain, a 2D

Table 3.1 The concentrations of various metabolites in the zebrafish brain extracts obtained by ^1H -NMR at 9.4T.

| Metabolites | Concentration ($\mu\text{mol/g}$) | Concentration relative to tCr |
|-------------|-------------------------------------|-------------------------------|
| tCr | 8.53 \pm 0.25 | 1.00 |
| GABA | 0.89 \pm 0.18 | 0.11 \pm 0.02 |
| Gln | 1.34 \pm 0.15 | 0.16 \pm 0.02 |
| Glu | 5.82 \pm 1.82 | 0.68 \pm 0.22 |
| ml | 2.01 \pm 0.26 | 0.24 \pm 0.03 |
| NAA | 5.43 \pm 1.15 | 0.64 \pm 0.14 |
| NAAG | 2.16 \pm 0.25 | 0.25 \pm 0.02 |
| Tau | 4.59 \pm 0.72 | 0.54 \pm 0.08 |
| Ala | 0.74 \pm 0.09 | 0.08 \pm 0.01 |
| Asp | 1.13 \pm 0.14 | 0.13 \pm 0.02 |
| Cho | 2.60 \pm 0.32 | 0.30 \pm 0.31 |
| GSH | 1.18 \pm 0.29 | 0.14 \pm 0.03 |
| HCar | 0.22 \pm 0.03 | 0.03 \pm 0.003 |
| Lac | 3.70 \pm 0.81 | 0.43 \pm 0.09 |

homonuclear (^1H - ^1H) dipolar correlation NMR spectrum was measured. The 2D homonuclear (^1H - ^1H) NMR spectrum played an important role in the identification, assignment and comparison of resonances of a large number of metabolites in zebrafish brain extracts. The spectrum clearly reveals separate correlation networks of several metabolites. On the basis of cross-peaks a full assignment of several brain metabolites was obtained (Fig. 3.5). Table 3.1 shows the concentration of various metabolites extracted from the brain of adult zebrafish.

3.5 Discussion

Zebrafish is increasingly used as a model organism for understanding brain diseases (5, 6, 14, 25, 26). The zebrafish brain has the same basic organization as other vertebrate brains (13) and there is a complex and well-developed dopaminergic system in the zebrafish (26, 27). Development of quantitative behavioural analysis methods for zebrafish and imaging systems of complete brain neurotransmitter networks at early embryonic stages have enabled comprehensive studies on these neurotransmitter systems in normal and pathological conditions (14). While the early zebrafish developmental stages are likely to be important in the future to analyze brain development and abnormalities produced by gene-knock-out methods, adult zebrafish with a full range of complex brain functions will probably have a significant role in analysis of generally important complex brain functions.

Although the organization of adult zebrafish brain has been studied in detail (10, 13), the metabolic composition of adult zebrafish brain is unknown. The brain metabolites are sensitive indicators of various pathological processes. The *in vivo* assessment of brain metabolites and tracking the

changes in metabolic profile over time will be indispensable tools to understand disease progression and its mechanism. In this study we applied and optimized the ^1H MRS sequence at high magnetic fields of 9.4T to get localized access to the zebrafish brain *in vivo*. Due to the very small size of zebrafish brain, we used an imaging coil of 10 mm to get good signal to noise ratio. To support imaging of living zebrafish, a mini-flow-through chamber was designed that could fit in a 10 mm volume coil (Fig. 1a). The combination of the optimized PRESS sequence, high field strength, strong gradient system, efficient water suppression and the use of short echo time allowed the measurement of high resolution spectra from a voxel as small as 3.3 μl placed in the middle of the zebrafish brain (Fig. 2). Good separation of resonances from various metabolites including NAA, Glu, Gln, Tau, tCr, Ins and PChl was achieved. The relative concentrations of various metabolites relative to tCr in zebrafish brain is shown in Fig. 3.3. The signals are broad when compared to previously reported *in vivo* spectra from various regions in the mouse brain which yield much narrower signals (28). This might be due to eddy currents and/or due to the difficulties in compensating for local magnetic field inhomogeneities in the small zebrafish head as compared to mouse brain.

An extensive metabolite profile and unambiguous resonance assignment of metabolites in zebrafish brain was obtained using the 2D COSY sequence (Fig. 5). The concentration of NAA was slightly lower in the brain extract than in the living zebrafish brain measured by *in vivo* MRS, which might be due to minor degradation during the extraction procedure. The concentrations of other metabolites such as Gln, Glu, mI and Tau in brain extracts were similar to the concentrations obtained *in vivo*. Since regional neurochemical information cannot be obtained in this study due to the small

size of zebrafish brain, a direct comparison of the metabolite profile of zebrafish brain to that of human brain cannot be made. However, in terms of the type of neurometabolites found in zebrafish brain we can conclude that zebrafish brain contains the same basic metabolic composition as found in other vertebrate brains, including human brain.

In conclusion, this study represents the first application of *in vivo* MRS to the zebrafish brain. A flow-through setup has been constructed and the high resolution localized MR pulse sequence has been optimized at 9.4T to get MR access to the small zebrafish brain. A localized MR spectrum from live zebrafish was obtained from a voxel as small as 3.3 μm . The composition of zebrafish brain which was completely unknown so far has been determined in this study for the first time using both *in vivo* and *in vitro* MRS. Future studies with a more advanced pulse sequence, better localization, and use of high magnetic field such as 17.6T may provide access to localized regions in the zebrafish brain. Further development of *in vivo* MRS for zebrafish brain could also include localized ^{31}P and ^{13}C MR spectroscopy which can be important for more extensive analysis of brain changes at the molecular level. The use of *in vivo* localized MRS in combination with μMRI in zebrafish brain can be useful for longitudinal studies to monitor biochemical changes during disease progression and treatment using various available zebrafish models in the near future.

Acknowledgements

We thank Fons Lefeber and Kees Erkelens for technical help concerning the μMRI and Annemarie Meijer for advice and providing the facility to work with the zebrafish. We thank Niels Braakman and Rob van de Ven for the help in using the LCModel data processing program. This work was partly

supported by grants from the Centre for Medical Systems Biology (CMSB) and CYTTRON within the Bsik program (Besluit subsidies investeringen kennisinfrastructuur) and Internationale Stichting Alzheimer Onderzoek (ISAO).

References

1. de Graaf RA. *In vivo* NMR spectroscopy: principles and techniques. 2nd edition. Chichester, West Sussex, England: John Wiley & Sons; 2007. p 43-95.
2. Rudin M, Beckmann N, Porszasz R, Reese T, Bochelen D, Sauter A. *In vivo* magnetic resonance methods in pharmaceutical research: current status and perspectives. *NMR Biomed* 1999;12:69-97.
3. Van der Linden A, Verhoye M, Pörtner HO, Bock C. The strengths of *in vivo* magnetic resonance imaging (MRI) to study environmental adaptational physiology in fish. *Magn Reson Mat Phys Biol Med* 2004;17:236-248.
4. Bock C, Satoris FJ, Pöter HO. *In vivo* MR spectroscopy and MR imaging on non-anaesthetized marine fish: techniques and first results. *Magn Reson Imag* 2002;20:165-172.
5. Bretaud S, Allen C, Ingham PW, Bandmann O. p53-dependent neuronal cell death in a DJ-1-deficit zebrafish model of Parkinson's disease. *J. Neurochem.* 2007;100:1626-1635.
6. Tomasiewicz HG, Flaherty DB, Soria JP, Wood JG. Transgenic zebrafish model of neurodegeneration. *J Neurosci Res* 2002;70:734-745.
7. Langenau DM, Zon LI. The Zebrafish: a new model of T-cell and thymic development. *Nat Rev Immunol* 2005;5:307-317.
8. Shin JT, Fishman MC. From Zebrafish to human: modular medical models. *Annu Rev Genomics Hum Genet* 2002;3:311-340.
9. Kabli S, Alia A, Spaink HP, Verbeek FJ, de Groot HJM. Magnetic resonance microscopy of the adult zebrafish. *Zebrafish* 2006;3:431-439.

10. Rupp B, Wullimann MF, Reichert H. The Zebrafish brain: a neuroanatomical comparison with the goldfish. *Anat Embryol* 1996;194:187-203.
11. Giraldez AJ, Cinalli RM, Glasner ME, Enright AJ, Thomsom JM, Baskerville S, Hammond SM, Bartell DP, Schier AF. MicroRNAs regulate brain morphogenesis in zebrafish. *Science* 2005;308:833-838.
12. Jeong JY, Kwon HB, Ahn JC, Kang D, Kwon SH, Park JA, Kim KW. Functional and developmental analysis of the blood-brain barrier in zebrafish. *Brain Res Bull* 2008;75:619-28.
13. Wullimann MF, Rupp B, Reichert H. Neuroanatomy of the zebrafish brain. Birkhauser-Verlag, Berlin; 1996. p144.
14. Panula P, Sallinen V, Sundvik M, Kolehmainen J, Torko V, Tittula A, Moshnyakov M, Podlasz P. Modulatory neurotransmitter systems and behavior: towards zebrafish models of neurodegenerative diseases. *Zebrafish* 2006;3:235-247.
15. Kerr JND, Denk W. Imaging *in vivo*: watching the brain in action. *Nat Rev Neurosci* 2008;9:195-205.
16. Westerfield M. The zebrafish book. A guide for the laboratory use of zebrafish (*Danio rerio*). 4th edition. University of Oregon Press; Eugene; 2000.
17. Suhartono L, Iren FV, de Winter W, Roytrakul S, Choi YH, Verpoorte R. Metabolic comparison cryopreserved and normal cells from *Tabernaemontana divaricata* suspension cultures. *Plant Cell Tissue Organ Culture* 2005; 83:59-66.
18. Henning J, Nauerth A, Friedburg H. RARE imaging: a fast imaging method for clinical MR. *Magn Reson Med* 1986; 3:823-833.
19. Gruetter R. Automatic, localized *in vivo* adjustment of all first- and second-order shim coils. *Magn Reson Med* 1993;29:804-811.
20. Bottomley PA. PRESS sequence. US Patent, 4 480 228 (1984).
21. Tkac I, Starcuk Z, Choi IY, Gruetter R. *In vivo* ¹H NMR spectroscopy of rat brain at 1 ms echo time. *Magn Reson Med* 1999;41:649-656.

22. Provencher SW. Estimation of metabolite concentrations from localized *in vivo* proton NMR spectra. *Magn Reson Med* 1993;30:672-679.
23. Provencher SW. Automatic quantisation of localized *in vivo* ^1H spectra with LCmodel. *NMR Biomed* 2001;14:260-264.
24. Pfeuffer J, Tkac I, Provencher SW, Gruetter R. Toward an *in vivo* neurochemical profile: quantification of 18 metabolites in short echo-time ^1H NMR spectra of the rat brain. *J Magn Reson* 1999;141:104–120.
25. Campbell WA, Yang H, Zetterberg H, Baulac S, Sears JA, Liu T, Stephen TCW, Zhong TP, Xia W. Zebrafish lacking Alzheimer presenilin enhancer 2 (Pen-2) demonstrate excessive p53-dependent apoptosis and neuronal loss. *J Neurochem*. 2006;96:1423-40.
26. Bai Q, Mullett SJ, Garver JA, Hinkle DA, Burton EA. Zebrafish DJ-1 is evolutionarily conserved and expressed in dopaminergic neurons. *Brain Res*. 2006;1113:33-44.
27. Ma PM, Lopez M. Consistency in the number of dopaminergic paraventricular organ-accompanying neurons in the posterior tuberculum of the zebrafish brain. *Brain Res*. 2003;967:267–272.
28. Tkac I, Henry PG, Andersen P, Keene CD, Low WC, Gruetter R. Highly resolved *in vivo* ^1H NMR spectroscopy of the mouse brain at 9.4 T. *Magn Reson Med* 2004;52:478-484.